P H Y S I C A L   R E V I E W   L E T T E R S

Thermodynamic Equilibrium Conditions of Graphene Films on SiC

Lydia Nemec, Volker Blum, Patrick Rinke, and Matthias Scheffler

Fritz-Haber-Institut der Max-Planck-Gesellschaft, Faradayweg 4-6, D-14195 Berlin, Germany
(Received 29 April 2013; published 6 August 2013)

First-principles surface phase diagrams reveal that epitaxial monolayer graphene films on the Si side of 3C-SiC(111) can exist as thermodynamically stable phases in a narrow range of experimentally controllable conditions, defining a path to the highest quality graphene films. Our calculations are based on a van der Waals corrected density functional. The full, experimentally observed $(6\sqrt{3} \times 6\sqrt{3})$-$R30°$ supercells for zero- to trilayer graphene are essential to describe the correct interface geometries and the relative stability of surface phases and possible defects.

The growth of wafer-size graphene films on a semiconducting substrate is a first step towards graphene-based electronics. On the semiconductor SiC, well-ordered graphene films can be grown directly by a simple process (Si sublimation from the surface; see, e.g., Refs. [1–7]) and the standard tools of semiconductor technology can be used for further manipulation. Indeed, graphene-based devices and even integrated circuits [8,9] have already been created on the Si side of SiC. However, controlling the precise thickness of graphene films is important to minimize the coexistence of monolayer graphene (MLG) and bilayer graphene (BLG) [3,5,10,11]. MLG areas exhibit no band gap, while BLG areas do [4]. A recent, joint experimental-theoretical study finds particularly high local resistances across monolayer-bilayer graphene junctions [12], a possible contributing factor to low carrier mobilities in graphene on SiC(0001) [3,12].

Growing graphene on SiC is special in the sense that, instead of offering C from the gas phase, graphene areas form by controlled Si sublimation from the surface [1,2]. Graphene films grown under ultrahigh vacuum conditions are typically inhomogeneous [3,5]. To improve their quality is therefore a major and ongoing experimental goal [3,5]. In the past, the appearance of different phases was often interpreted [5,13,14] as intuitive, successive intermediates formed by an outgoing Si flux, ultimately leading to bulklike graphite layers. If graphene films of various thicknesses were a result of a purely kinetically limited Si sublimation process (controlled by growth temperature and time), improving upon the homogeneity of the layer thickness would be difficult. It would be helpful if there were a set of thermodynamic equilibrium conditions (e.g., temperature T and partial pressures p of Si and C [15]) at which a desired film thickness was thermodynamically stable over all others. As long as T is sufficiently high to

overcome the relevant kinetic barriers, large-scale ordered films of that thickness could then be formed simply by finding and maintaining (p, T) near these equilibrium conditions.

Indeed, experimental evidence is mounting that controlled (p, T) conditions do aid the growth of graphene on SiC. Reference [16] shows that the carbon-rich "zero-layer graphene" (ZLG) or "buffer layer" precursor phase [1,2,13,17] (not yet graphene) on the Si face is a reversible thermodynamic equilibrium phase at high T and controlled disilane background pressure. Reversibility is much harder to demonstrate once a complete graphene plane is formed [18], but an increased growth temperature in an Ar buffer gas leads to much improved MLG film homogeneity [3]. Wafer-size MLG films are also reported for growth in a confined cavity that may retain a finite Si background pressure as Si evaporates from the surface [5]. Finally, a well-defined graphene precursor phase on the C face at finite disilane background pressure was reported recently [6]. What is still not clear, however, is whether MLG itself is an equilibrium phase under certain conditions. If so, one could ideally facilitate the growth of MLG but not BLG on SiC(111).

We here present first-principles theoretical evidence that such equilibrium conditions indeed exist for MLG (and, possibly, even BLG) on the Si face of SiC(111). We employ density-functional theory (DFT) using the van der Waals (vdW) corrected [19] Perdew-Burke-Ernzerhof (PBE) functional [20] (PBE + vdW). Strategies to include vdW effects are an active field (see, e.g., Refs. [21–26] and references therein). However, for the complex carbon-rich interfaces of interest here, the present incorporation of vdW terms [19] reflects the state of the art and no unambiguously quantitatively improved approach exists to our knowledge. For the relevant bulk phases, the impact of different standard functionals is well understood and systematic. Predicted lattice parameters (see also Supplemental Material [27]) for 3C-SiC are within 1% of experiment: $a_{3C\text{-SiC}} = 4.33$ Å [local density approximation (LDA)], 4.38 Å (PBE without vdW correction), 4.36 Å (PBE + vdW), and 4.36 Å (experiment [28]). Similarly small

discrepancies arise for diamond C and for the in-plane lattice parameter of graphite: $a_{\text{graphite}} = 2.45$ Å (LDA), 2.47 Å (PBE), and 2.46 Å (PBE + vdW). Zero-point corrections (ZPC) to the lattice parameters are also below 1% (see the Supplemental Material [27]). For the interplanar lattice parameter c of graphite, vdW effects must be included into the PBE functional (6.65 Å for LDA, 6.66 Å for PBE + vdW, but 8.65 Å for PBE). All our calculations use the FHI-aims all-electron code [29,30] with "tight" numerical settings and the massively parallel ELPA eigensolver library [31] to guarantee accurate total energies for the very large structure sizes involved (see the Supplemental Material for details [27]).

In experiment, one encounters a series of phases on the Si side of 3C-SiC(111) [experimentally also observed on 4H-SiC(0001) and 6H-SiC(0001)] when going from Si-rich to C-rich conditions. In UHV, a (3×3) Si-rich layer [32] can be prepared. Upon Si sublimation, a simpler $(\sqrt{3} \times \sqrt{3})$-$R30°$ bulk-terminated surface with one adsorbed Si adatom per three unit cells follows [33,34]. Removing yet more Si creates a partially covalently bonded carbon layer, the ZLG phase, with a large, commensurate unit cell: one (13×13) honeycomb graphene-like supercell on a $(6\sqrt{3} \times 6\sqrt{3})$-$R30°$ mesh of the SiC substrate [1]. Compared to a graphene plane in graphite, the lattice match is almost strain free [experiment: 0.2% at $T = 0$ K [28,35], PBE + vdW: 0.1% (see the Supplemental Material [27])]. The ZLG phase does not yet exhibit the electronic properties of actual freestanding graphene [13]. Further heating detaches the ZLG C plane from the substrate to form MLG and a new C-rich layer underneath [36,37]. This process can be continued to successively form BLG [38] and multilayer graphene films. Importantly, our calculations address the graphenelike films in their experimentally observed, large commensurate $(6\sqrt{3} \times 6\sqrt{3})$-$R30°$ supercells, using slabs containing six Si-C bilayers under each reconstructed phase [1742 up to 2756 atoms for ZLG up to three-layer graphene (3LG)]. The top three SiC bilayers and all planes above are fully relaxed (residual energy gradients 8×10^{-3} eV/Å or less).

Figures 1(a)–1(c) show ZLG, MLG, and BLG together with key geometry parameters predicted at the PBE + vdW level. Since all planes are corrugated [39–41], histograms for the atomic z coordinates are included. The interface geometry stays essentially the same as more graphene planes are added. For MLG, we see a significant buckling of the topmost graphene layer (≈ 0.41 Å between highest and lowest atoms). This buckling is qualitatively consistent with existing STM images [11,42,43]. In BLG, the corrugation is slightly reduced. The two top planes are buckled by 0.24 Å and 0.32 Å, respectively. This buckling reflects some coupling to the covalently bonded C-rich interface plane, which is much more corrugated (≈ 0.8 Å in our work, similar to experimental estimates [44,45]). The observed graphene interplanar distances near the interface
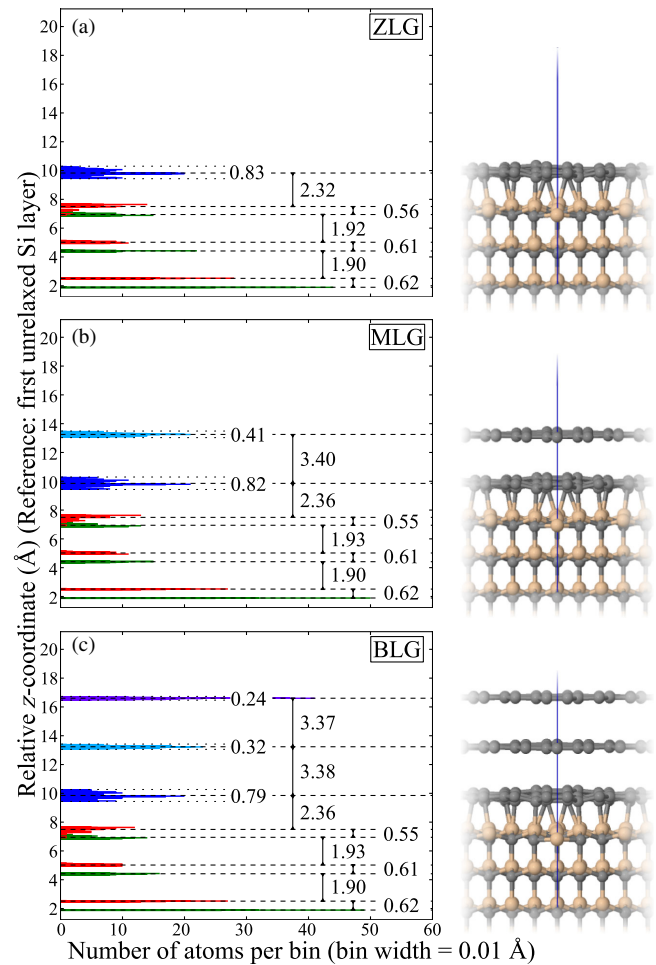

FIG. 1 (color online). (a)–(c): PBE + vdW calculated geometry of ZLG, MLG, and BLG on Si face 3C-SiC(111) and histograms of atomic z coordinates (bin width: 0.01 Å) relative to the fourth SiC bilayer.

are slightly expanded compared to experimental bulk graphite (3.34 Å [35]) and in good qualitative agreement with estimates from scanning tunneling microscopy [43] and transmission electron microscopy [46].

We have also compared our findings to geometries for the straight PBE functional (no vdW correction), and for the LDA. In PBE, the C-C interplanar distances are unphysically expanded (4.42 Å for MLG). In contrast, the LDA geometry of the carbon planes agrees qualitatively with PBE + vdW, although LDA incorporates no long-range vdW interactions. The first qualitative geometry difference between PBE + vdW and LDA appears in the Si part of the top SiC bilayer, where some Si atoms (those with dangling bonds pushing against the π-bonded parts of the C interface plane [47]) are located much deeper (by ≈ 0.3 Å) in PBE and PBE + vdW than in LDA. A direct crystallographic verification would be desirable.

In a grand canonical formalism, equilibrium conditions for different surface phases can be represented by the

chemical potentials of C and Si, μ_C and μ_{Si}. In experiment, μ_C and μ_{Si} can be manipulated, e.g., through the substrate temperature and background pressure [5,6,15,16] of gases that supply Si or C [48]. Consider the surface energies γ of a two-dimensional periodic SiC slab with a C face and a Si face. In the limit of sufficiently thick slabs, we have

$$\gamma_{\text{Si-face}} + \gamma_{\text{C-face}} = \frac{1}{A}(E^{\text{slab}} - N_{Si}\mu_{Si} - N_C\mu_C). \quad (1)$$

N_{Si} and N_C denote the number of Si and C atoms in the slab, respectively. A is the chosen area. We report surface energies in electron volts per (1×1) SiC unit cell area. The letter E denotes total energies for a given atomic geometry throughout this work. In all calculations, we choose a fixed H-terminated C-face geometry, which cancels out for all Si-face related surface energy differences.

It is important to note that Eq. (1) defines thermodynamic equilibrium conditions, but no conditions regarding growth kinetics. Thus, potential kinetic barriers do not enter the definition of thermodynamic stability according to the lowest surface energy given by Eq. (1). Of course, the actual surface morphology that forms in practice (finite growth time) still depends on temperature and the nature of kinetic barriers (see, e.g., Ref. [14] and references therein). For instance, higher growth temperatures that facilitate lateral surface diffusion processes are cited as the reason for improved graphene film quality in Refs. [3,16]. Still, Eq. (1) matters, since it will be much more difficult to drive a surface to a desired nonequilibrium phase than to an actual equilibrium phase.

The major experimental (T, p) dependence during growth arises through the reservoirs of Si and C, which define μ_{Si} and μ_C [15,16] (a small possible contribution of finite T stresses at the growth conditions [49] must be kept in mind) [50]. Thus, a precise control of background gases as reservoirs (e.g., disilane [16]) is desirable, even if calibration variations [51] may require specific (T, p) ranges to be adjusted for a given growth chamber.

In equilibrium with a stable SiC bulk, μ_C and μ_{Si} are linked through

$$\mu_{Si} + \mu_C = 2E^{\text{bulk}}_{SiC} = E^{\text{bulk}}_C + E^{\text{bulk}}_{Si} + 2\Delta H_f(\text{SiC}). \quad (2)$$

The energies are per atom. $\Delta H_f(\text{SiC})$ is the formation enthalpy of SiC with respect to elemental C and Si. The bulk phases define the chemical potential limits within which the SiC crystal is stable against decomposition into bulk Si or C: $\mu_C \leq E^{\text{bulk}}_C$ and $\mu_{Si} \leq E^{\text{bulk}}_{Si}$, leading to

$$E^{\text{bulk}}_C + \Delta H_f(\text{SiC}) \leq \mu_C \leq E^{\text{bulk}}_C \quad (3)$$

and analogous for Si. The diamond structure for Si is the appropriate bulk phase. For C, there is a close competition between diamond and graphite [52,53]. We thus include both phases in our analysis.

The experimentally reported energy difference between diamond and graphite at $T = 0$ K is 25 meV/atom [52]. Based on the potential energy minima (no ZPC), graphite is more stable than diamond in PBE + vdW by 60 meV/atom [see Fig. 2(a)]. This is qualitatively consistent with the extrapolated experimental phase hierarchy. In plain PBE graphite is overstabilized by 130 meV/atom. In LDA, both phases are similarly stable: considering only the potential energy surface, diamond is slightly more stable (by 12 meV), but already the inclusion of ZPC [53] would neutralize this balance (graphite more stable by 3 meV/atom [54]).

Figure 2(a) shows the surface energies of the known surface phases of SiC (Si face) as a function of $\Delta\mu_C = \mu_C - E^{\text{bulk}}_C$ for PBE + vdW. The most stable phase for a given value of $\Delta\mu_C$ is that with the lowest surface energy. Going through Fig. 2(a) from left to right, we find the expected broad stability ranges for the Si-rich (3×3) and $(\sqrt{3} \times \sqrt{3})$-$R30°$ phases. Just before the C-rich limit (bulk graphite), there is a crossover first to ZLG, then to MLG, and even to a very narrow slice of the BLG phase. Finally, ABA-stacked 3LG crosses BLG within 1 meV of bulk graphite.
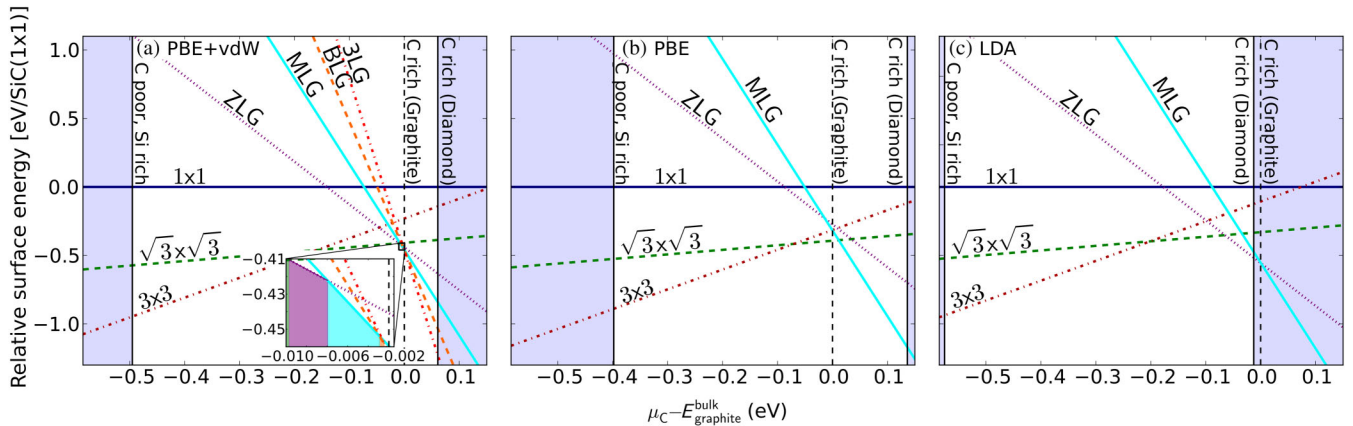

FIG. 2 (color online).   Surface energies of different phases of Si-face 3C-SiC(111) relative to (1×1), vs μ_C. Areas outside the limits set by Eq. (3) are shaded. (a) PBE + vdW, (b) PBE, (c) LDA.

While the stability ranges are narrow (see the inset of Fig. 2(a): 4 meV, 5 meV, and <1 meV for ZLG, MLG, and BLG, respectively, at the chemical potential axis), it is important to recall that this does not necessarily imply narrow experimental conditions: a drastic change in the number of Si (N_{Si}) and C (N_C) atoms can correspond to a small change of μ. For instance, one would first have to remove all Si from the SiC crystal to go beyond the graphite stability line in equilibrium. However, the surface-energy differences between the different phases are also rather small (a few tens of milli electron volts per (1×1) SiC surface unit cell). The primary approximations that we cannot systematically improve in our calculations are possible small temperature-dependent surface strain effects [49] and the density functional itself. For instance, correlation effects beyond standard semilocal DFT render the Si-rich ($\sqrt{3} \times \sqrt{3}$)-$R30°$ adatom phase nonmetallic [55–57], whereas semilocal DFT gives a metallic interface. Similar Si dangling bonds exist under the ZLG interface. Here, too, the question of a metallic (semilocal DFT) [58] vs (almost) nonmetallic interface in angle-resolved photoemission spectroscopy [13,59] has been raised. If so, this nonmetallicity could lead to small shifts in the surface energetics and thus in the phase diagram. Since all phases in question should experience some small additional stabilization, the impact on the relative stability may be even smaller, but current parameter-free density functionals cannot decide to which degree. The key message of Fig. 2(a) is thus that MLG and its related phases all appear at least as very near equilibrium phases, a fact that is nonetheless critical for a qualitatively correct understanding of their growth and properties.

What we can do is to show how our results would be affected by different density functionals. We have thus recomputed the surface phase diagram up to MLG for two widely used functionals in Figs. 2(b) and 2(c): plain PBE and LDA. As expected, the absence of vdW tails in plain PBE changes the phase diagram drastically. Due to the overstabilization of graphite, its stability line moves significantly further to the left, as does the crossover point between ZLG and MLG. Therefore, neither ZLG nor MLG becomes stable over the competing Si-rich ($\sqrt{3} \times \sqrt{3}$)-$R30°$ phase in PBE, in contradiction to experiment [16]. In the LDA, the most significant change compared to PBE + vdW is the apparent incorrect stability hierarchy of graphite vs diamond (without ZPC). If the diamond line is discounted, our calculations show the ZLG-MLG crossover point almost exactly on the graphite line. Still, even taking LDA at face value implies the existence of T-p conditions very close to equilibrium for MLG, making the experimental search for such conditions promising.

Figure 2 thus shows the most important point of our Letter: the existence of equilibrium or near-equilibrium chemical potential ranges for ZLG, MLG, and even BLG, corresponding to specific T/p conditions in

experiment. This finding proves the potential for much better growth control than what could be expected if each phase were just a necessary (but not thermodynamically stable) kinetic intermediate. While true reversibility for actual MLG may be hard to achieve [16,18] (the reverse growth process, disassembling a fully formed graphene plane, would be kinetically difficult), the forward growth process from MLG to BLG under Si out diffusion should still be limitable by appropriate T/p conditions. A macroscopically homogeneous surface very close to pure-phase MLG should thus be achievable in principle.

Figure 2 shows unambiguously the importance of a consistently accurate numerical treatment of the experimentally observed phases in their large unit cells. It would obviously be much more economical to consider smaller-cell approximant phases to the true ($6\sqrt{3} \times 6\sqrt{3}$)-$R30°$ supercells. However, the residual artificial strain and inadequate bonding in those phases are too large for meaningful surface energy comparisons [60]. For instance, the popular ($\sqrt{3} \times \sqrt{3}$)-$R30°$ [47,61] approximant would intersect the graphite stability line at a surface energy $\gamma|_{\mu_C = E_{graphite}^{bulk}} = 0.15$ eV, far above the actually stable phases. Likewise, a slightly rotated (5×5) approximant to ZLG [62] (a periodicity sometimes seen in experiment [17,63]) would intersect at ($\gamma|_{\mu_C = E_{graphite}^{bulk}} = -0.35$ eV), higher by 0.06 eV than even the closest competing Si-rich phase, the ($\sqrt{3} \times \sqrt{3}$)-$R30°$ Si adatom phase ($\gamma|_{\mu_C = E_{graphite}^{bulk}} = -0.41$ eV). The (5×5) phase is either a nonequilibrium phase, or its structure is not the same as that assumed in Ref. [62].

The true problem with artificially strained approximant phases is that their strain can obscure other electronically relevant properties, such as the energetics of defects. As an example, we consider a C-rich defect type suggested as an equilibrium feature of the ZLG phase in Ref. [58]. Two different defect positions, "hollow" and "top," were proposed [58]. Indeed, both would be more stable than the hypothetical ($\sqrt{3} \times \sqrt{3}$)-$R30°$ ZLG approximant when included there in a (3×3) arrangement as done in Ref. [58]: -1.75 eV per defect for the hollow position, -2.93 eV per defect for top, both at $\mu_C = E_{graphite}^{bulk}$. However, the same defects are unstable when included into and compared to the correct ($6\sqrt{3} \times 6\sqrt{3}$)-$R30°$ ZLG phase: $+5.28$ eV per defect for the hollow position, $+5.27$ eV for the top position, again at $\mu_C = E_{graphite}^{bulk}$ (see the Supplemental Material [27] for more details).

In conclusion, we can now rationalize some specific growth-related observations. In UHV, the background pressures of Si and C are low and ill defined, leading to inferior morphologies and wide variations of experimental conditions [51,64]. Much more homogeneous growth can be achieved in an Ar atmosphere [3] or by controlling the Si background pressure by a disilane reservoir [16] or a confined cavity [5]. Maintaining a controlled Si partial

pressure at constant, higher temperature than allowed in UHV is most likely the important step. Similar considerations may also aid the much more difficult growth of MLG on the C face [5,65], where a well-defined interface layer at finite disilane pressure was proposed [6]. Near-equilibrium surface conditions may indeed be the key to the best possible epitaxial growth of graphene on SiC.

---

[1] A. Van Bommel, J. Crombeen, and A. Van Tooren, Surf. Sci. **48**, 463 (1975).

[2] I. Forbeaux, J.-M. Themlin, and J.-M. Debever, Phys. Rev. B **58**, 16396 (1998).

[3] K. V. Emtsev, A. Bostwick, K. Horn, J. Jobst, G. L. Kellogg, L. Ley, J. L. McChesney, T. Ohta, S. A. Reshanov, J. Röhrl et al., Nat. Mater. **8**, 203 (2009).

[4] C. Riedl, C. Coletti, and U. Starke, J. Phys. D **43**, 374009 (2010).

[5] W. A. de Heer, C. Berger, M. Ruan, M. Sprinkle, X. Li, Y. Hu, B. Zhang, J. Hankinson, and E. Conrad, Proc. Natl. Acad. Sci. U.S.A. **108**, 16 900 (2011).

[6] N. Srivastava, G. He, Luxmi, and R. M. Feenstra, Phys. Rev. B **85**, 041404 (2012).

[7] G. R. Yazdi, R. Vasiliauskas, T. Iakimov, A. Zakharov, M. Syväjärvi, and R. Yakimova, Carbon **57**, 477 (2013).

[8] Y. Lin, A. Valdes-Garcia, S. Han, D. Farmer, I. Meric, Y. Sun, Y. Wu, C. Dimitrakopoulos, A. Grill, P. Avouris et al., Science **332**, 1294 (2011).

[9] S. Hertel, D. Waldmann, J. Jobst, A. Albert, M. Albrecht, S. Reshanov, A. Schöner, M. Krieger, and H. Weber, Nat. Commun. **3**, 957 (2012).

[10] C. Berger, Z. Song, T. Li, X. Li, A. Ogbazghi, R. Feng, Z. Dai, A. Marchenkov, E. Conrad, N. Phillip et al., J. Phys. Chem. B **108**, 19 912 (2004).

[11] P. N. First, W. A. de Heer, T. Seyller, C. Berger, J. A. Stroscio, and J.-S. Moon, MRS Bull. **35**, 296 (2011).

[12] S.-H. Ji, J. B. Hannon, R. M. Tromp, V. Perebeinos, J. Tersoff, and F. M. Ross, Nat. Mater. **11**, 114 (2011).

[13] K. V. Emtsev, F. Speck, T. Seyller, L. Ley, and J. D. Riley, Phys. Rev. B **77**, 155303 (2008).

[14] F. Ming and A. Zangwill, Phys. Rev. B **84**, 115459 (2011).

[15] K. Reuter and M. Scheffler, Phys. Rev. B **65**, 035406 (2001).

[16] R. M. Tromp and J. B. Hannon, Phys. Rev. Lett. **102**, 106104 (2009).

[17] C. Riedl, U. Starke, J. Bernhardt, M. Franke, and K. Heinz, Phys. Rev. B **76**, 245406 (2007).

[18] J. B. Hannon (private communication).

[19] A. Tkatchenko and M. Scheffler, Phys. Rev. Lett. **102**, 073005 (2009).

[20] J. P. Perdew, K. Burke, and M. Ernzerhof, Phys. Rev. Lett. **78**, 1396 (1997).

[21] S. Grimme, Comput. Mol. Sci. **1**, 211 (2011).

[22] M. Dion, H. Rydberg, E. Schröder, D. C. Langreth, and B. I. Lundqvist, Phys. Rev. Lett. **92**, 246401 (2004).

[23] K. Lee, É. D. Murray, L. Kong, B. I. Lundqvist, and D. C. Langreth, Phys. Rev. B **82**, 081101 (2010).

[24] J. Klimes, D. R. Bowler, and A. Michaelides, J. Phys. Condens. Matter **22**, 022201 (2010).

[25] G. X. Zhang, A. Tkatchenko, J. Paier, H. Appel, and M. Scheffler, Phys. Rev. Lett. **107**, 245501 (2011).

[26] A. Tkatchenko, R. A. DiStasio, R. Car, and M. Scheffler, Phys. Rev. Lett. **108**, 236402 (2012).

[27] See Supplemental Material at http://link.aps.org/supplemental/10.1103/PhysRevLett.111.065502. The Supplemental Material includes reference data for the numerical convergence of our calculations, calculated lattice parameters, and other cohesive properties of the bulk reference phases 3C-SiC, diamond Si, diamond and graphite C, without and with zero-point corrections for the functionals used here, and structural details of the defects as introduced in Ref. [58].

[28] Z. Li and R. C. Bradt, J. Mater. Sci. **21**, 4366 (1986).

[29] V. Blum, R. Gehrke, F. Hanke, P. Havu, V. Havu, X. Ren, K. Reuter, and M. Scheffler, Comput. Phys. Commun. **180**, 2175 (2009).

[30] V. Havu, V. Blum, P. Havu, and M. Scheffler, J. Comput. Phys. **228**, 8367 (2009).

[31] T. Auckenthaler, V. Blum, H. Bungartz, T. Huckle, R. Johanni, L. Krämer, B. Lang, H. Lederer, and P. Willems, Parallel Comput. **37**, 783 (2011).

[32] U. Starke, J. Schardt, J. Bernhardt, M. Franke, K. Reuter, H. Wedler, K. Heinz, J. Furthmüller, P. Käckell, and F. Bechstedt, Phys. Rev. Lett. **80**, 758 (1998).

[33] R. Kaplan, Surf. Sci. **215**, 111 (1989).

[34] U. Starke, J. Schardt, J. Bernhardt, M. Franke, and K. Heinz, Phys. Rev. Lett. **82**, 2107 (1999).

[35] Y. Baskin and L. Meyer, Phys. Rev. **100**, 544 (1955).

[36] T. Seyller, A. Bostwick, K. Emtsev, K. Horn, L. Ley, J. McChesney, T. Ohta, J. Riley, E. Rotenberg, and F. Speck, Phys. Status Solidi B **245**, 1436 (2008).

[37] J. B. Hannon, M. Copel, and R. M. Tromp, Phys. Rev. Lett. **107**, 166101 (2011).

[38] T. Ohta, A. Bostwick, T. Seyller, K. Horn, and E. Rotenberg, Science **313**, 951 (2006).

[39] S. Kim, J. Ihm, H. J. Choi, and Y. W. Son, Phys. Rev. Lett. **100**, 176802 (2008).

[40] F. Varchon, P. Mallet, J.-Y. Veuillen, and L. Magaud, Phys. Rev. B **77**, 235412 (2008).

[41] G. Sclauzero and A. Pasquarello, Phys. Rev. B **85**, 161405 (R) (2012).

[42] W. Chen, H. Xu, L. Liu, X. Gao, D. Qi, G. Peng, S. C. Tan, Y. Feng, K. P. Loh, and A. T. S. Wee, Surf. Sci. **596**, 176 (2005).

[43] C. Berger, J. Veuillen, L. Magaud, P. Mallet, V. Olevano, M. Orlita, P. Plochocka, C. Faugeras, G. Martinez, M. Potemski et al., Int. J. Nanotechnology **7**, 383 (2010).

[44] S. Goler, C. Coletti, V. Piazza, P. Pingue, F. Colangelo, V. Pellegrini, K. V. Emtsev, S. Forti, U. Starke, F. Beltram et al., Carbon **51**, 249 (2013).

[45] L. H. de Lima, A. de Siervo, R. Landers, G. A. Viana, A. M. B. Goncalves, R. G. Lacerda, and P. Häberle, Phys. Rev. B **87**, 081403(R) (2013).

[46] W. Norimatsu and M. Kusunoki, Chem. Phys. Lett. **468**, 52 (2009).

[47] F. Varchon, R. Feng, J. Hass, X. Li, B. Nguyen, C. Naud, P. Mallet, J. Veuillen, C. Berger, E. Conrad *et al.*, Phys. Rev. Lett. **99**, 126805 (2007).

[48] From a microscopic point of view, as long as the Si diffusion path to the outside (sublimation) remains kinetically accessible, so does the inward diffusion path, and near equilibrium with a Si reservoir gas can be achieved. During intermediate stages of the formation of a new graphene plane [46], such diffusion paths must be available.

[49] J. Roehrl, M. Hundhausen, K. Emtsev, T. Seyller, R. Graupner, and L. Ley, Appl. Phys. Lett. **92**, 201918 (2008).

[50] In principle, we could include the much smaller (p, T) dependence of the solid phases by focusing on Gibbs free energies $G(T, p)$ in the (quasi)harmonic approximation instead of E. However, quantifying this T dependence precisely would here necessitate accurate phonon calculations for structure sizes of the order of ≈ 2000 atoms, a task that is computationally prohibitive at present. ZPC are small for the bulk phases (see the Supplemental Material [27]).

[51] W. Lu, J. J. Boeckl, and W. C. Mitchell, J. Phys. D **43**, 374004 (2010).

[52] R. Berman and F. Simon, Z. Elektrochem.: Ber. Bunsenges. Phys. Chem. **59**, 333 (1955).

[53] M. T. Yin and M. L. Cohen, Phys. Rev. B **29**, 6996 (1984).

[54] F. Lazarevic, L. Nemec, V. Blum, and M. Scheffler (to be published).

[55] J. E. Northrup and J. Neugebauer, Phys. Rev. B **52**, R17001 (1995).

[56] M. Rohlfing and J. Pollmann, Phys. Rev. Lett. **84**, 135 (2000).

[57] F. Bechstedt and J. Furthmüller, J. Phys. Condens. Matter **16**, S1 721 (2004).

[58] Y. Qi, S. H. Rhim, G. F. Sun, M. Weinert, and L. Li, Phys. Rev. Lett. **105**, 085502 (2010).

[59] K. Emtsev, T. Seyller, F. Speck, L. Ley, P. Stojanov, J. Riley, and R. Leckey, Mater. Sci. Forum **556–557**, 525 (2007).

[60] G. Sclauzero and A. Pasquarello, Diam. Relat. Mater. **23**, 178 (2012).

[61] A. Mattausch and O. Pankratov, Phys. Rev. Lett. **99**, 076802 (2007).

[62] O. Pankratov, S. Hensel, and M. Bockstedte, Phys. Rev. B **82**, 121416 (2010).

[63] U. Starke and C. Riedl, J. Phys. Condens. Matter **21**, 134016 (2009).

[64] P. Sutter, Nat. Mater. **8**, 171 (2009).

[65] J. Hass, R. Feng, J. E. Millán-Otoya, X. Li, M. Sprinkle, P. N. First, W. A. de Heer, E. H. Conrad, and C. Berger, Phys. Rev. B **75**, 214109 (2007).